Table S 1. Overview of PHILEAS flights including flight times, duration and objectives.

Flight Nr.	Take off - Landing [UTC]	Duration [h]	From - To	Objectice
F01	09:16 -12:38 (3.92)	3.92	EDMO-EDMO	EMV flight
F02	07:04 - 15:47	8.87	EDMO-EDMO	Undiluted ASM air masses and westward eddy shedding
F03	09:10 - 10:31	1.48	EDMO-EDMO	Turbulence calibration
F04	07:35 - 15:09	7.73	EDMO-EDMO	Background air with little ASM influence
F05	07:05 - 15:02	8.17	EDMO-EDMO	Undiluted ASM air masses and westward eddy shedding
F06	06:56 - 14:39	7.92	EDMO-EDMO	Old background air with little ASM influence over Sweden, Subtropical air masses over Italy
F07	08:40 - 20:42	10.92	EDMO-BIKF-PANC	Transfer flight to Anchorage with stop in Island
F08	17:57 - 02:14	8.60	PANC-PANC	Air with large ASM fraction, in-mixing into the lower stratosphere
F09	18:18 - 02:55	8.95	PANC-PANC	Extreme wildfires in Canada, Revisit air mass with large ASM fraction (F08)
F10	16:07 - 03:46	11.17	PANC-PADK-PANC	Air mass with large ASM fraction over the Pacific, combine 3D tomographic remote-sensing (hexagon) and in-situ measurements.
F11	21:17 - 03:52	7.20	PANC-PANC	Air masses from tomographic hexagon (F10), filamentation and mixing of ASM air
F12	18:04 - 02:12	8.43	PANC-PANC	Stratospheric background, (aged) wildfire plumes
F13	18:02 - 03:05	9.32	PANC-PANC	Two distinguished air masses with high ASM fraction, Tomography of air masses to be revisited (F14 Mainz)
F14	19:58 - 05:03	9.28	PANC-PANC	Re-visit distinguished air masses with a large ASM contribution
F15	18:02 - 02:55	9.15	PANC-PANC	Re-visit the distinguished air mass with large ASM fraction (F14 Mainz) after in-mixing into lower stratosphere
F16	21:58 - 07:12	9.48	PANC-PANC	Slanted filament of Asian monsoon air over the Pacific at different altitudes. Shear zones (TSL) in the vicinity of the jet
F17	22:06 - 06:23	8.63	PANC-PANC	Follow-up of F16, monsoon filaments from previous day
F18	17:54 - 02:41	9.03	PANC-PANC	Sample background, re-sample air from F17
F19	21:55 - 07:17	9.68	PANC-EDMO	Transfer flight
F20	07:38 - 16:07	8.68	EDMO-EDMO	Background flight at end of the monsoon season

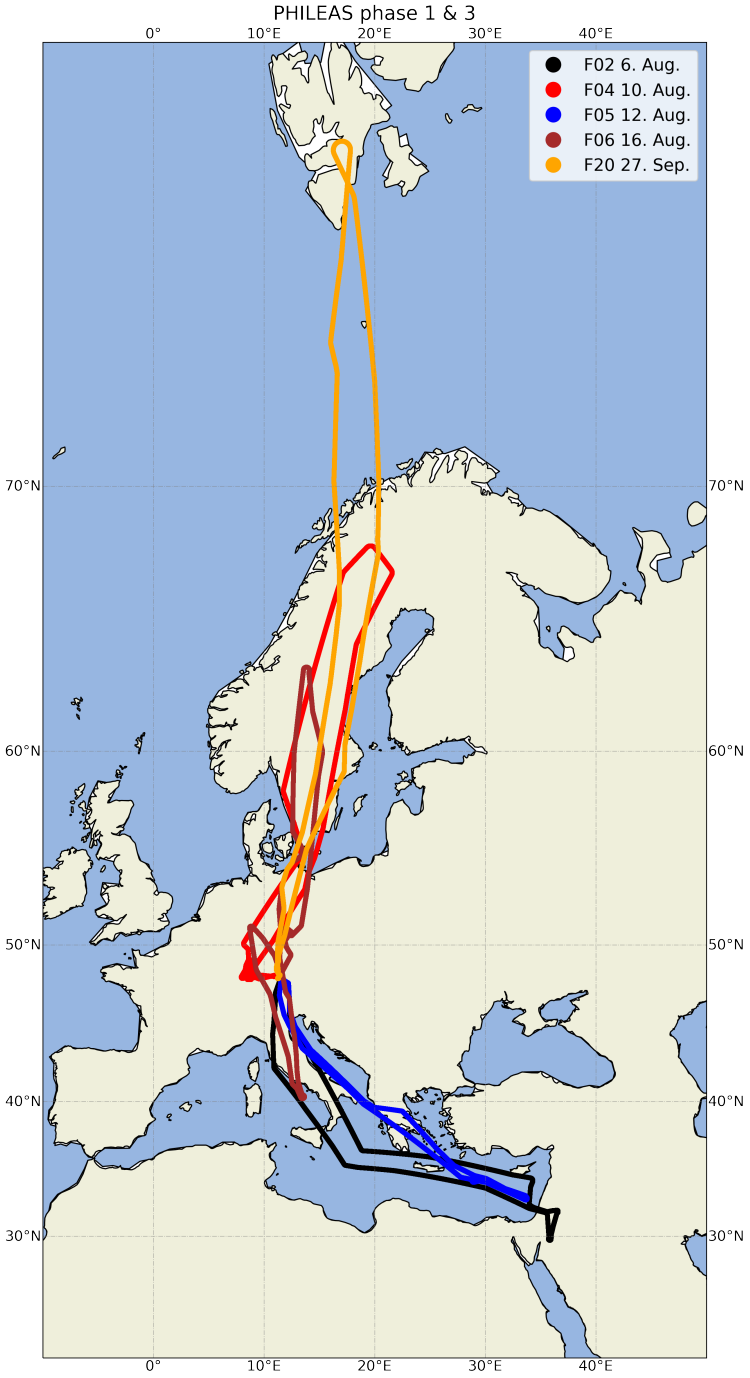

Figure S 1. Flight tracks of the first and third phase of PHILEAS.

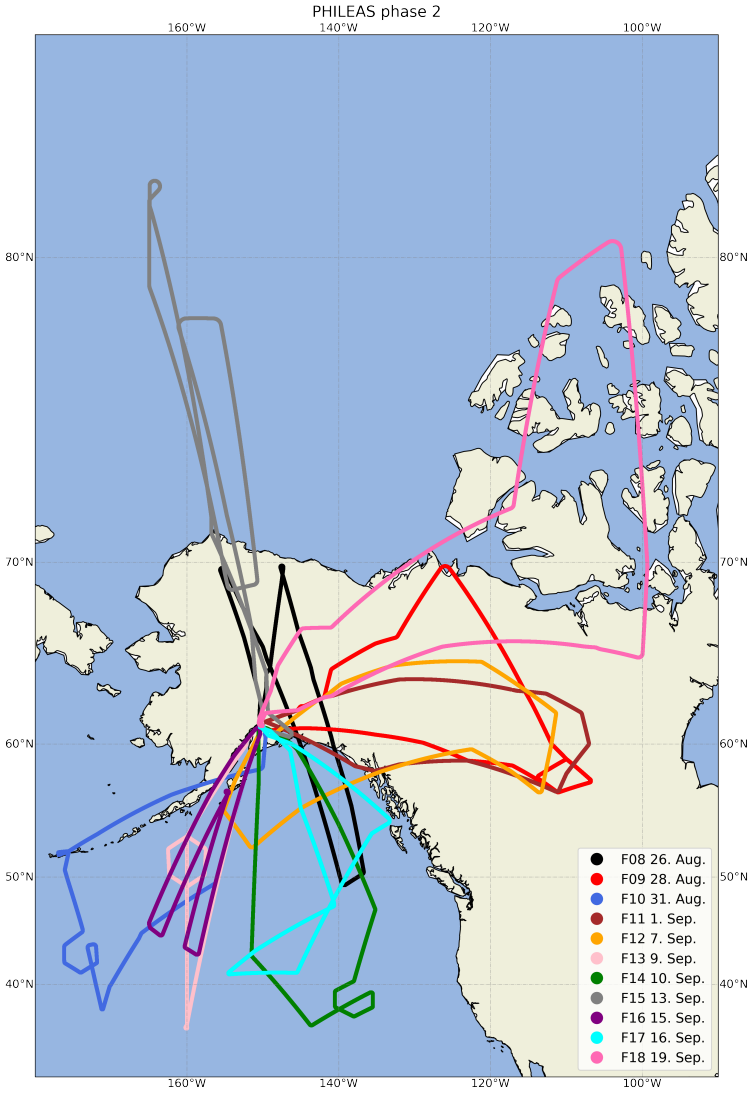

Figure S 2. Flight tracks of the second phase of PHILEAS.

Figure S 3. Flight tracks of the transfer flights of PHILEAS.

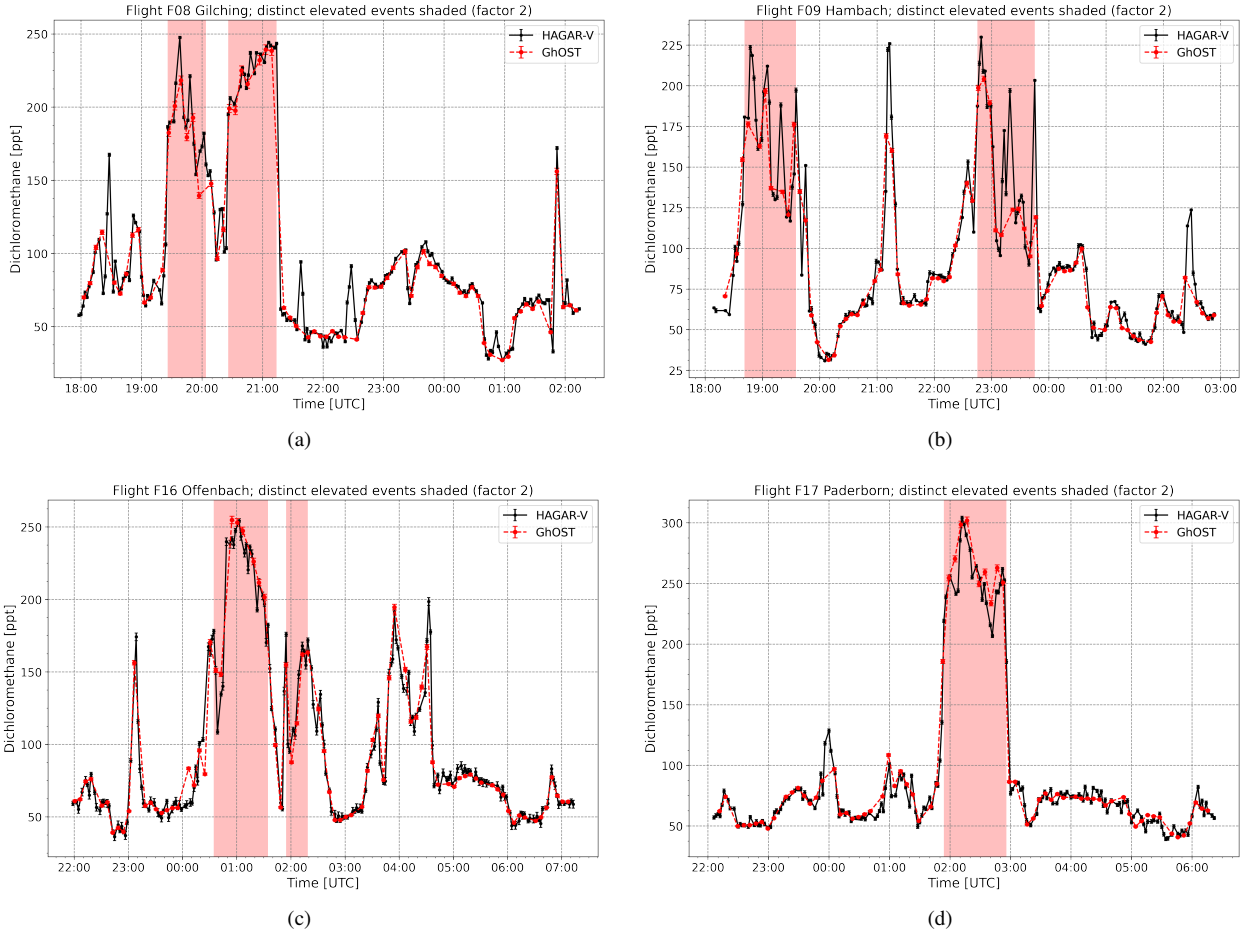

Figure S 4. Time series of CH_2Cl_2 from the GhOST (red) and HAGAR-V (black) instrument, with elevated events shaded in red (factor 2 larger than background).

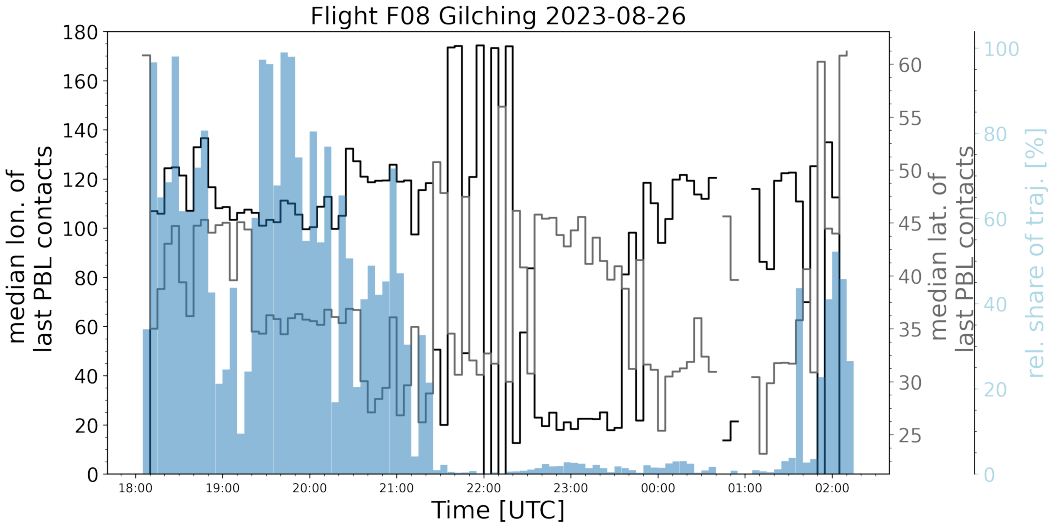

Figure S 5. Flight F08 FLEXPART median latitude in grey and longitude in black of particles within the 5-min intervals. Proportion of trajectories within respective 5-minute intervals shown in blue, arriving at the PBL during the 12-day backward analysis.

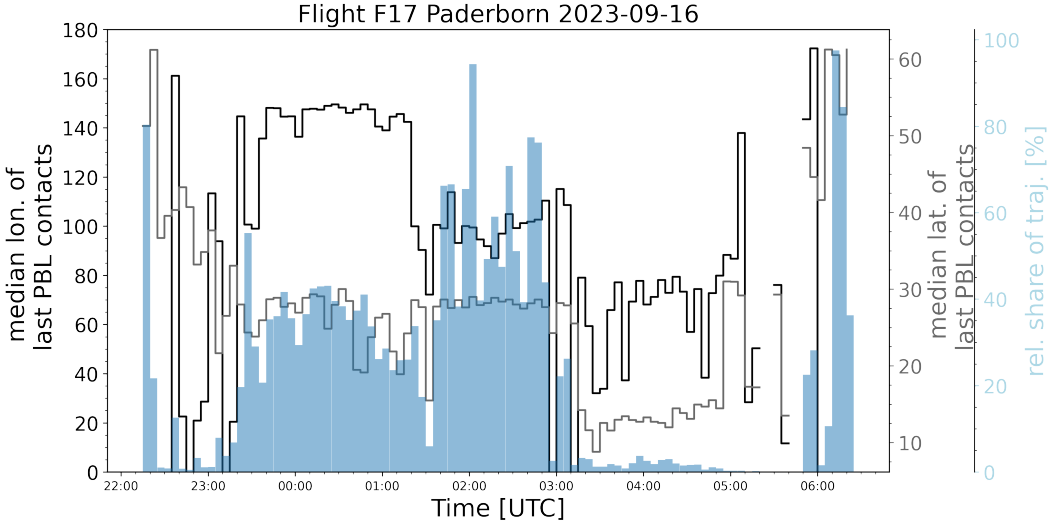

Figure S 6. like Fig. S 5 but for flight F17.

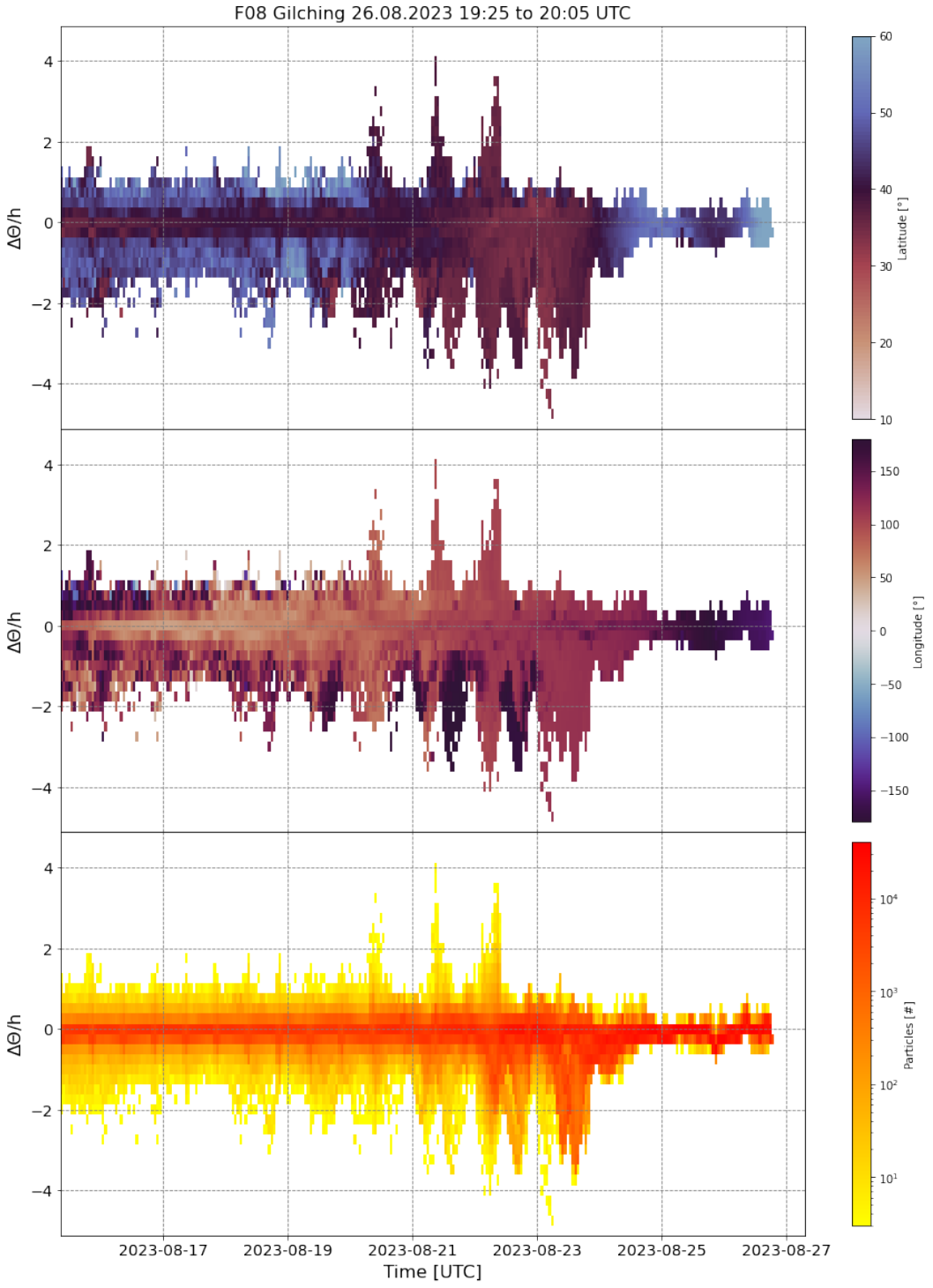

Figure S 7. Hourly fluctuations in potential temperature observed along particle trajectories within the 12 days backward calculation for the first event on flight F08. Top row shows color code according to latitude, middle row according to longitude, and bottom according to particle density.

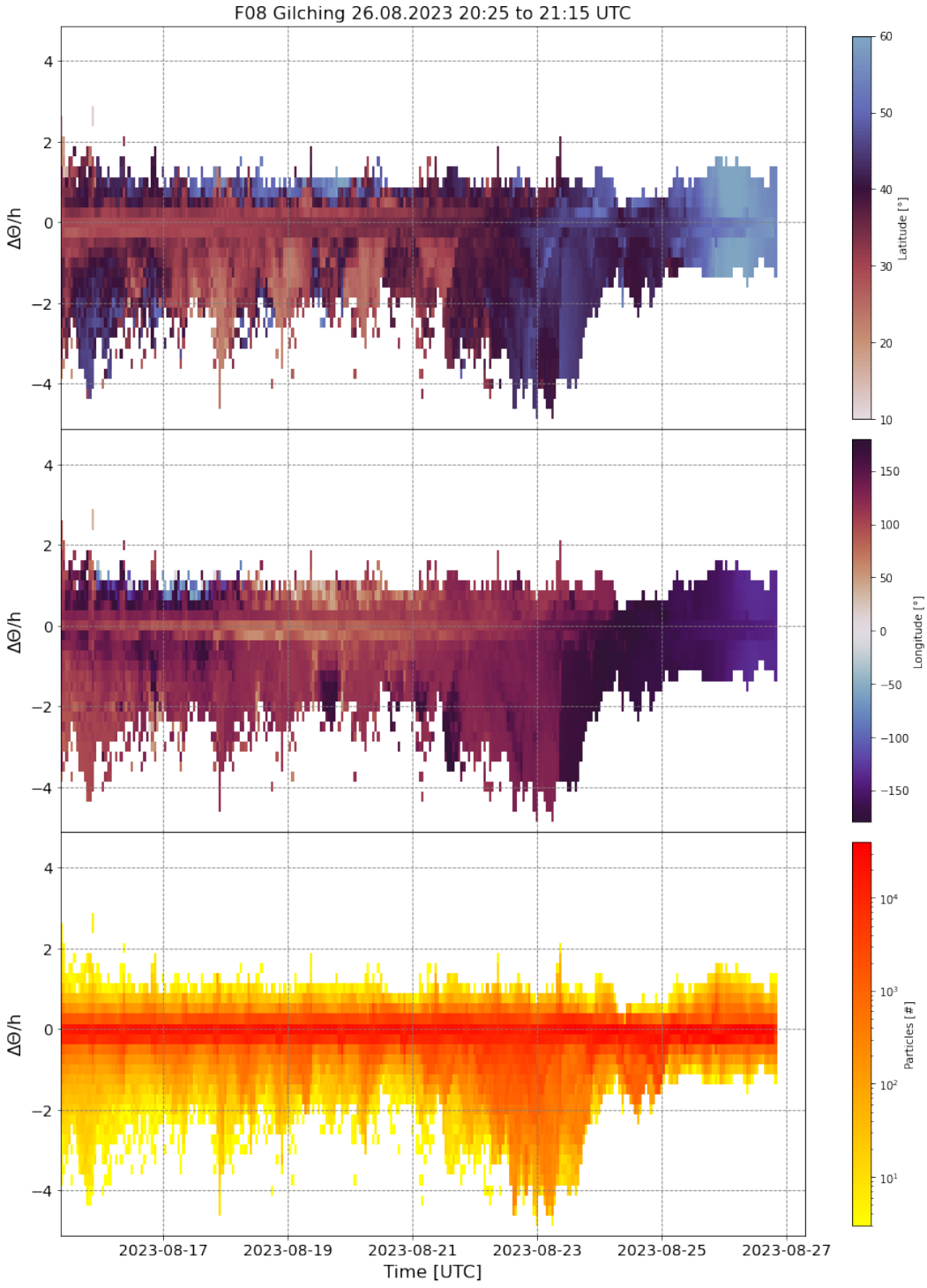

Figure S 8. like Fig. S 7 but for the second event on flight F08.

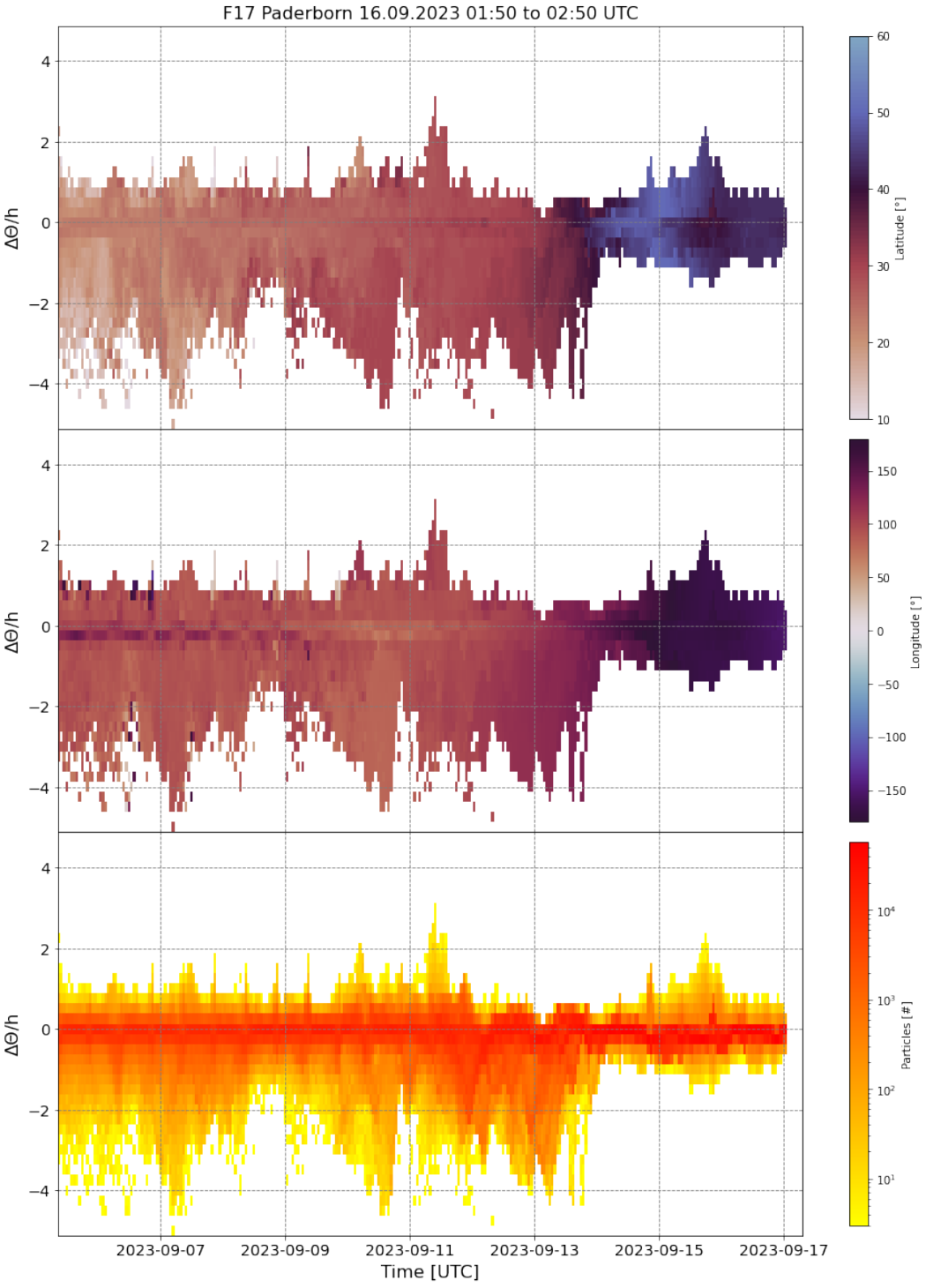

Figure S 9. like Fig. S 7 but for the event on flight F17.

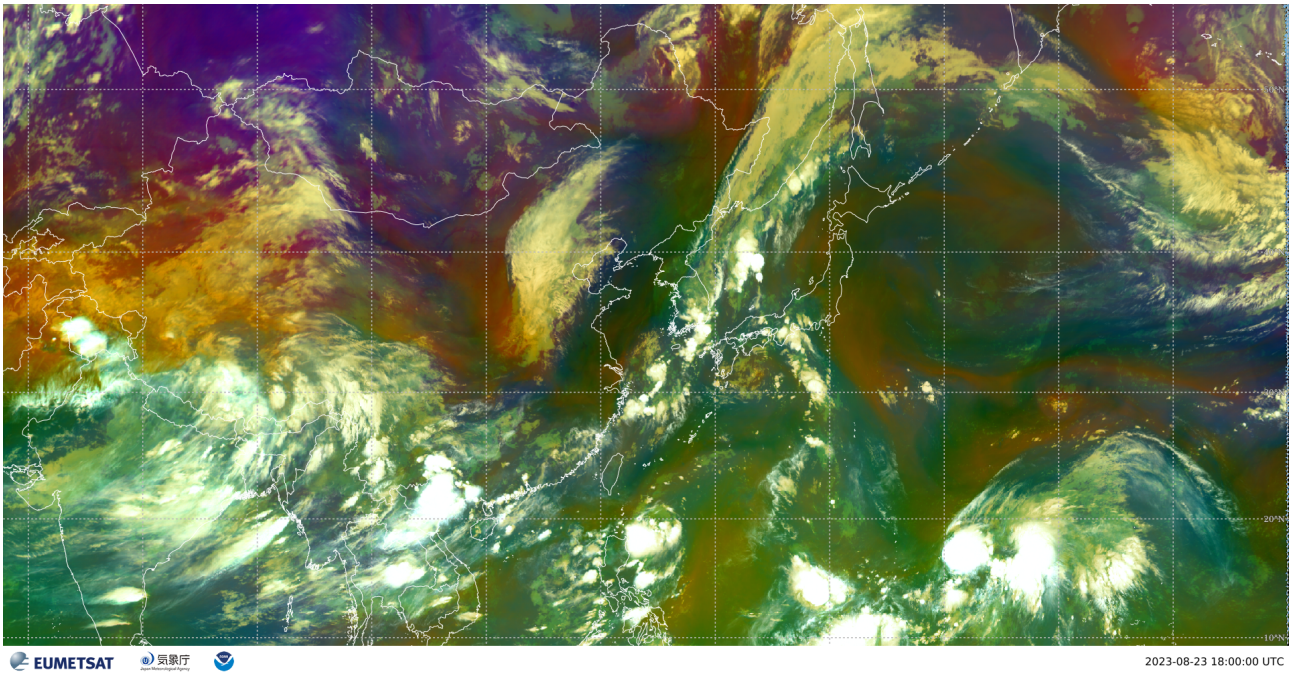

Figure S 10. RGB Airmass satellite image for 18 UTC on August 23, 2023. The RGB Airmass satellite image uses the two water vapour and the ozone absorption channels. The WV6.2–WV7.3 difference (red colour beam), the IR9.7–IR10.8 difference (green colour beam), and the WV6.2 (blue colour beam). This image helps to distinguish air masses and high-reaching multi-layered clouds and to analyse dynamic processes in the atmosphere. ©EUMETSAT [2024]

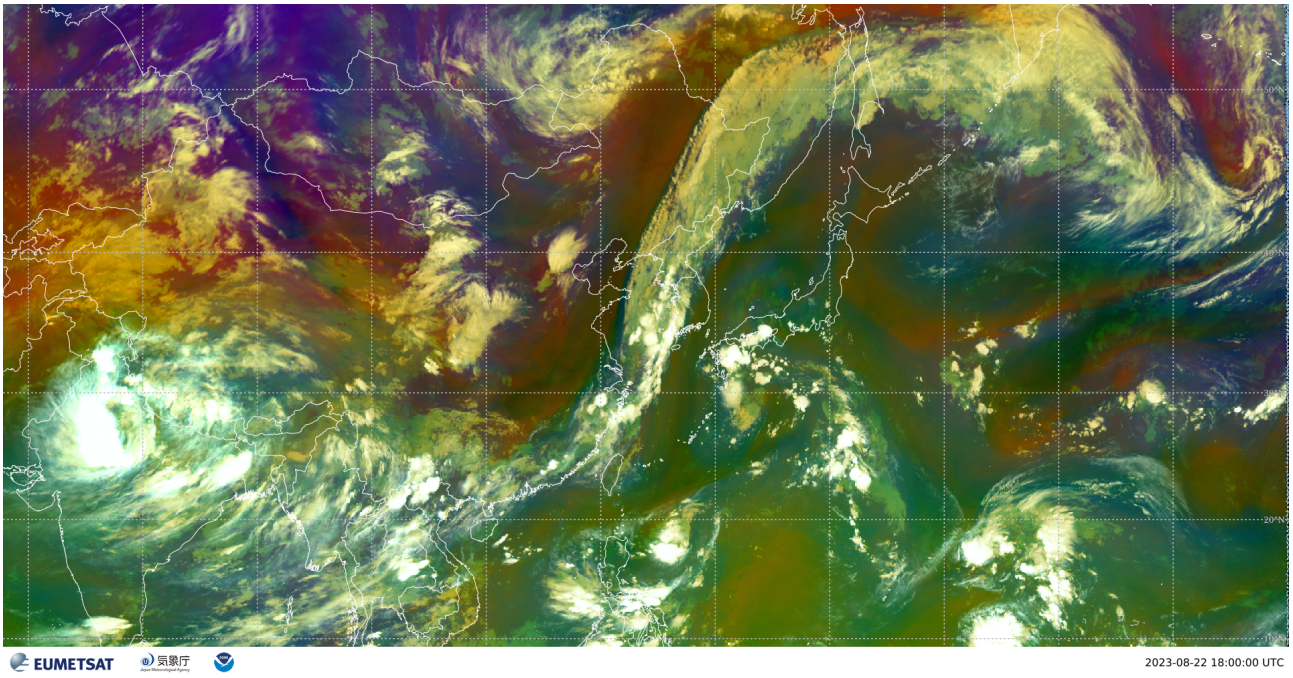

Figure S 11. like Fig. S 10 but for for 18 UTC on August 22, 2024.

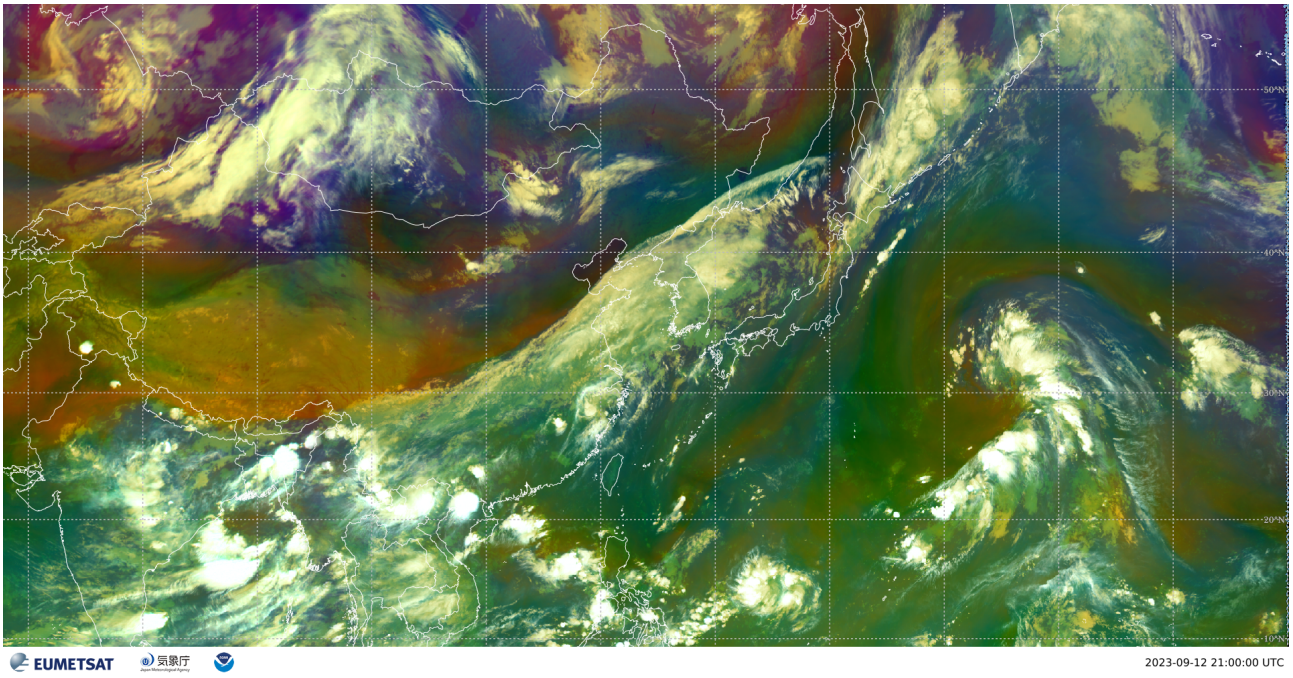

Figure S 12. like Fig. S 10 but for for 21 UTC on September 12, 2024.

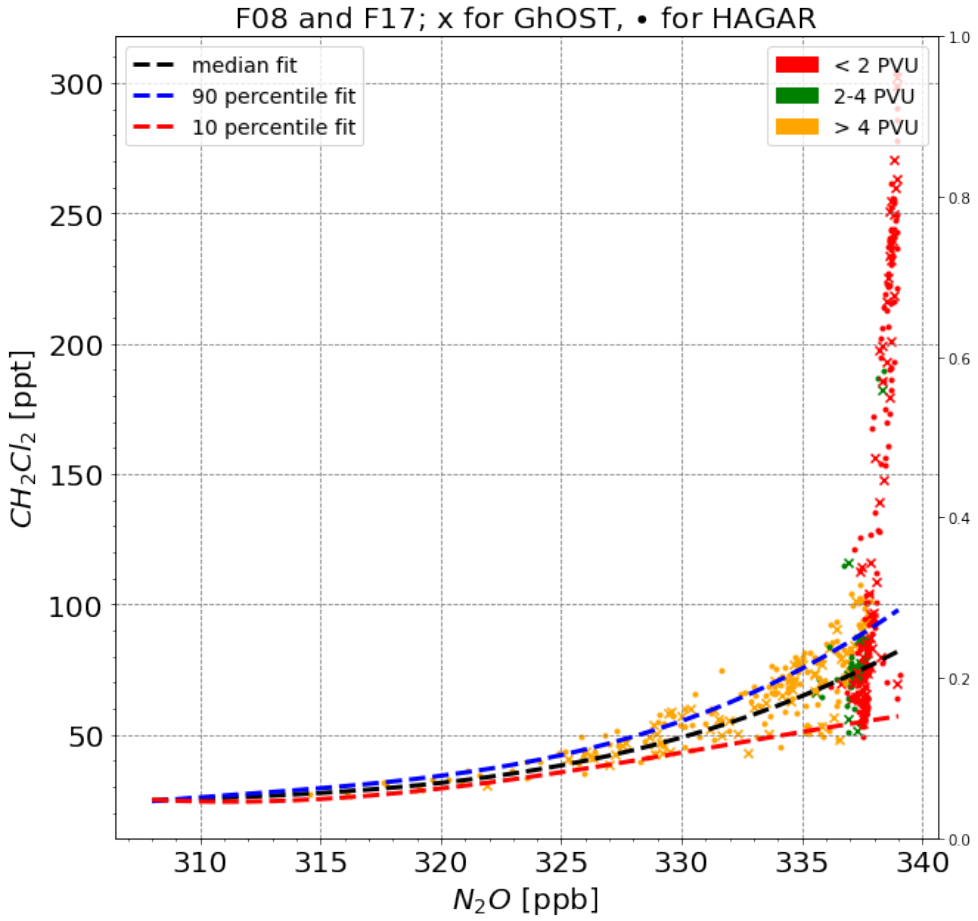

Figure S 13. CH_2Cl_2-N_2O relationship for flight F08 and F17, color coded by PVU ranges. Crosses for HAGAR-V and points for GhOST.

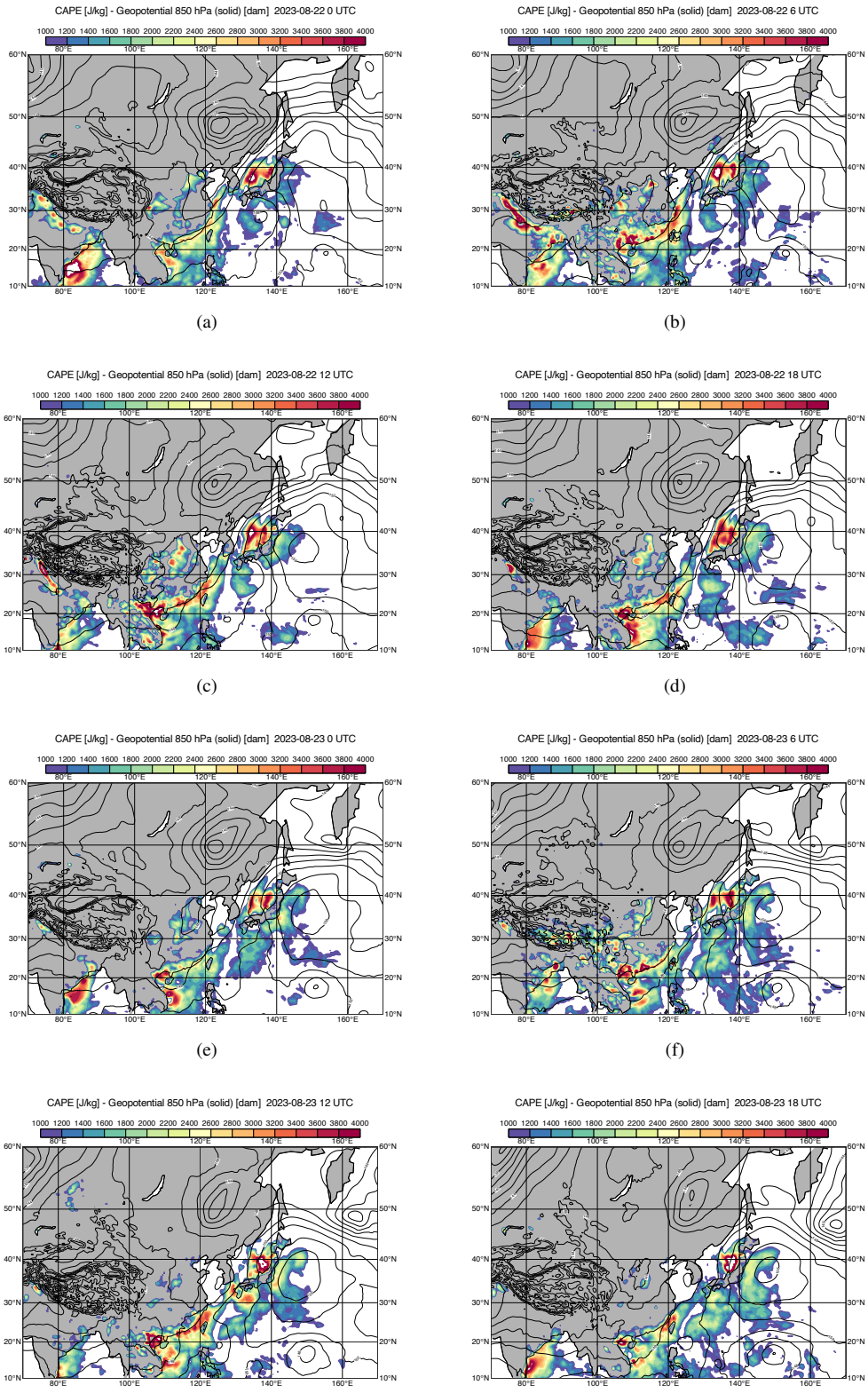

Figure S 14. Vertical distribution of the Convective Available Potential Energy (CAPE) and 850 hPa geopotential data for August 22 and 23, presented in 6-hourly intervals.

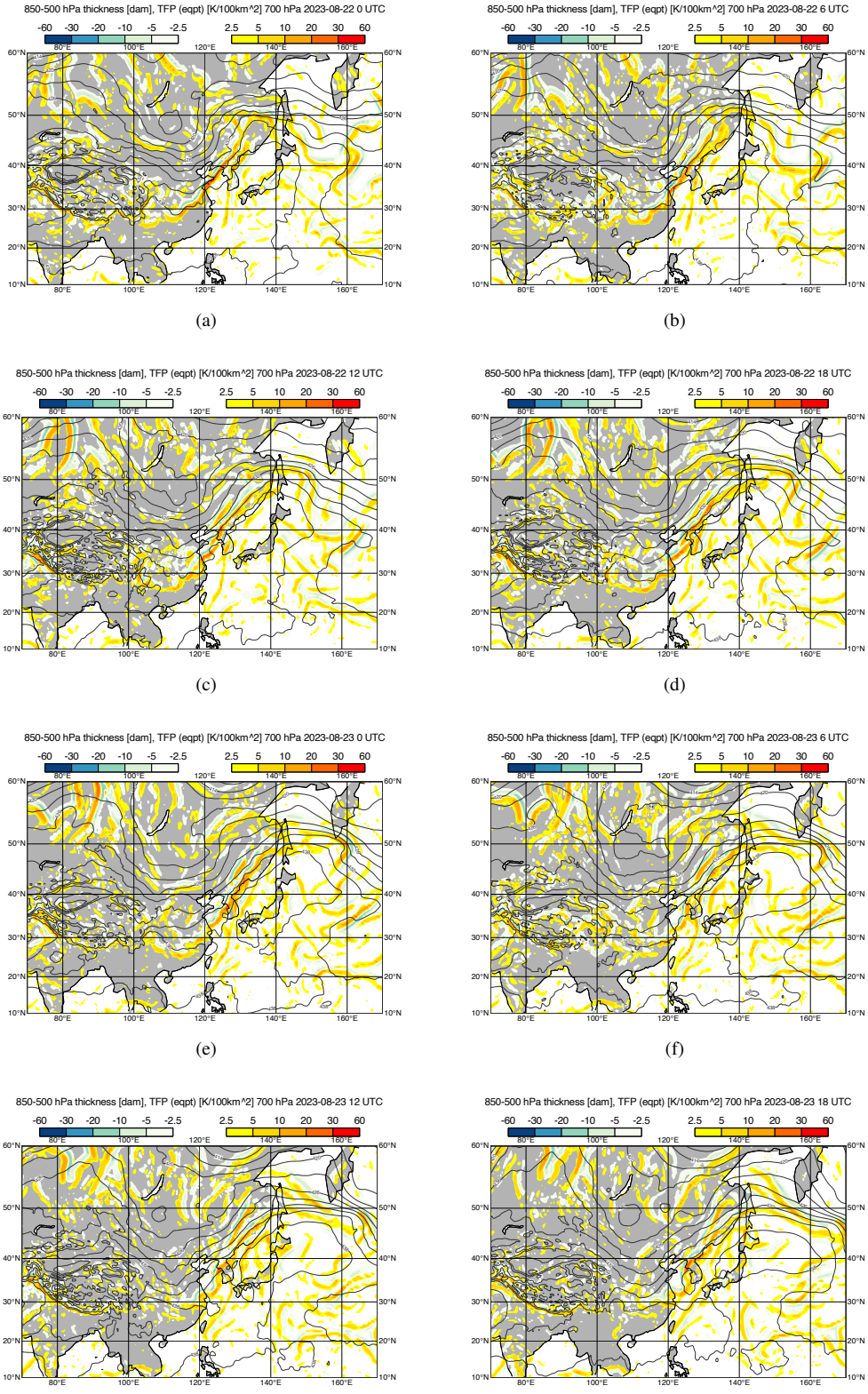

Figure S 15. The thermal front parameter (TFP) and 850–500 hPa thickness data for August 22 and 23, presented in 6-hourly intervals.

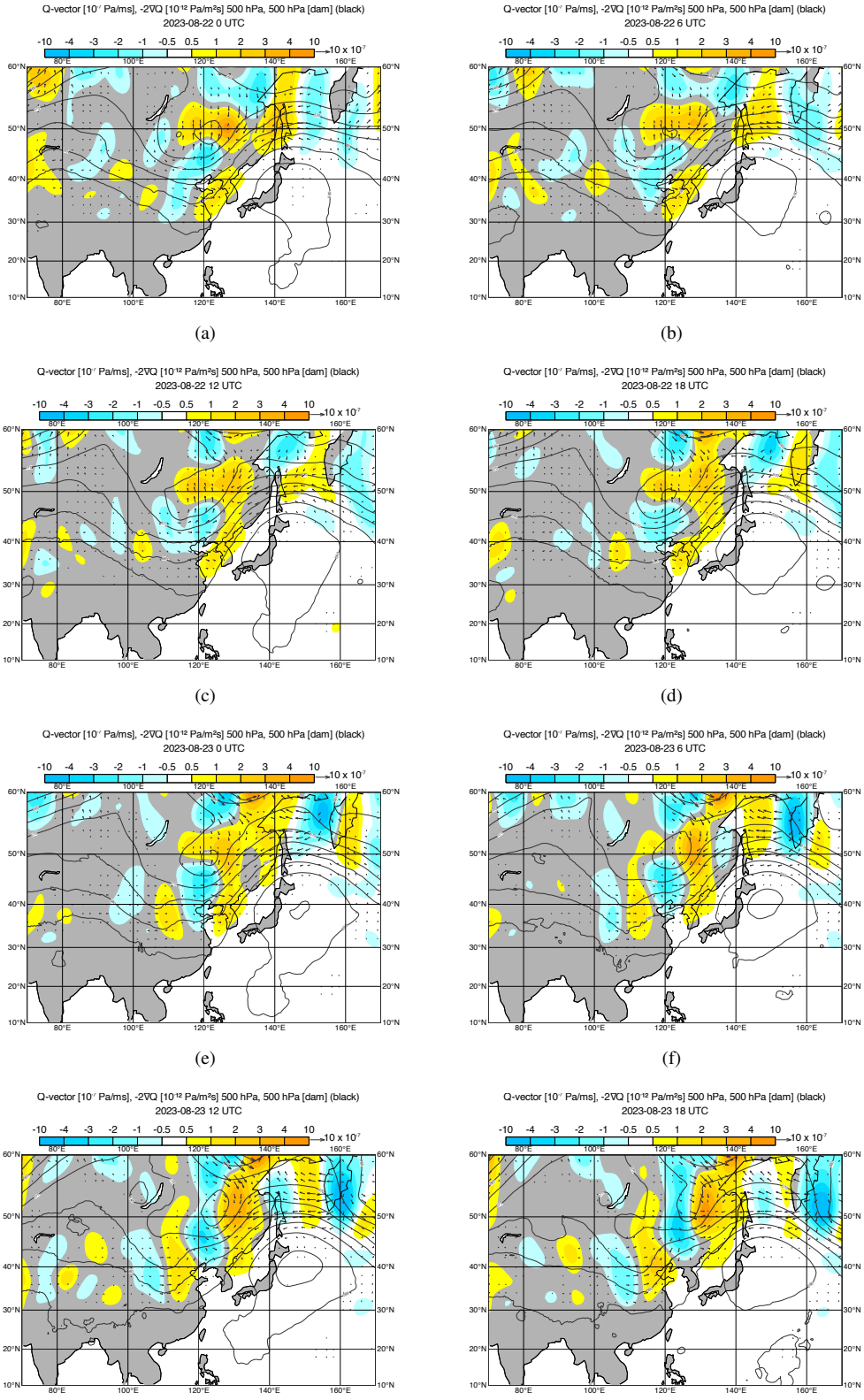

Figure S 16. Q- Vector, Q-Vector vergences, and 500 hPa geopotential data for August 22 and 23, presented in 6-hourly intervals.

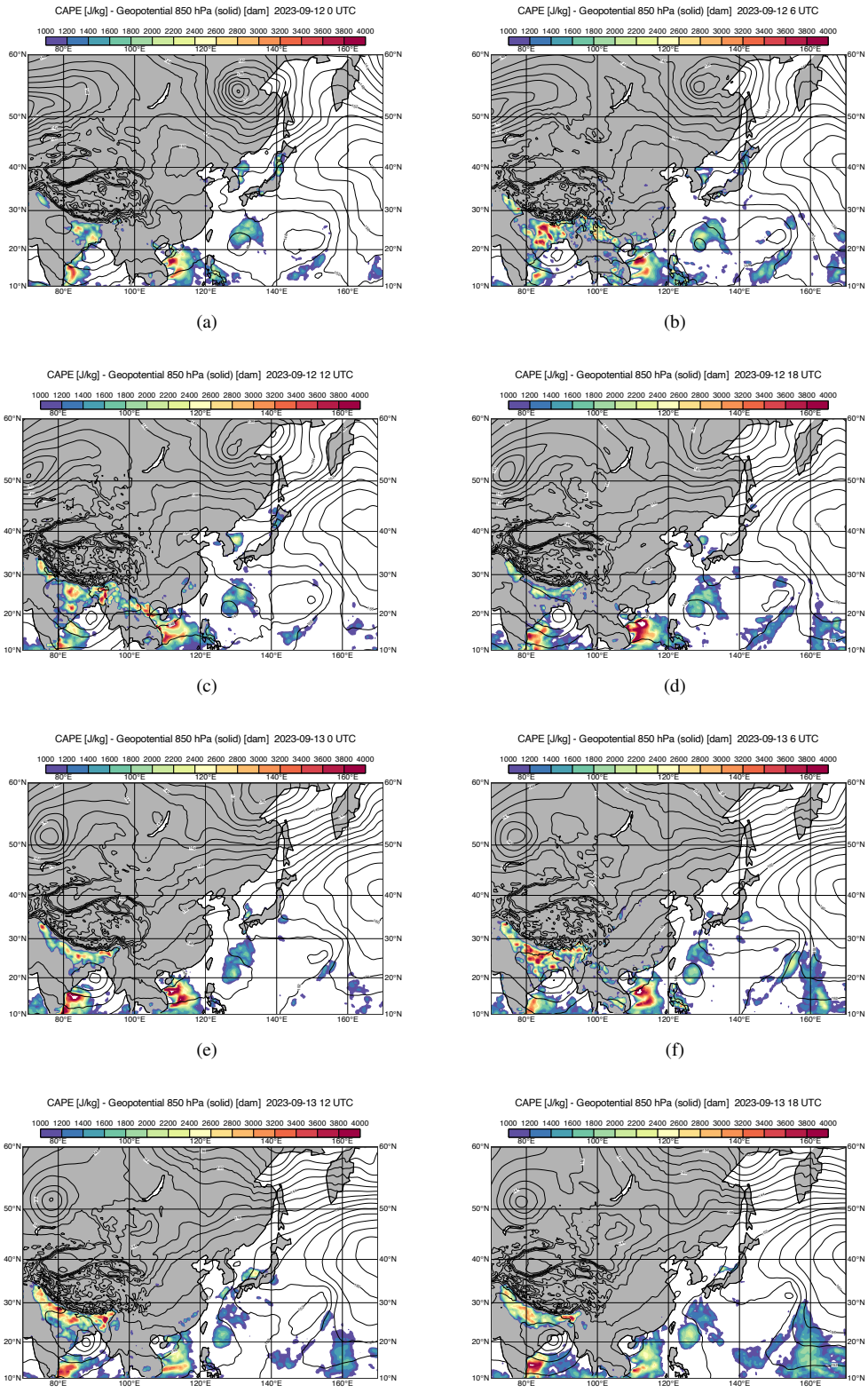

Figure S 17. Vertical distribution of the Convective Available Potential Energy (CAPE) and 850 hPa geopotential data for September 12 and 13, presented in 6-hourly intervals.

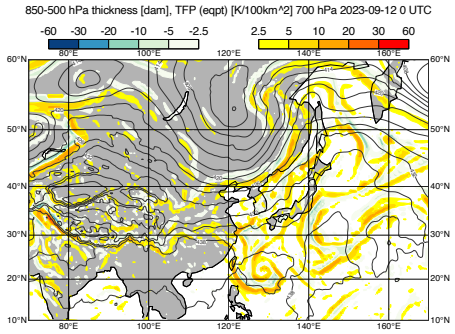

(a)

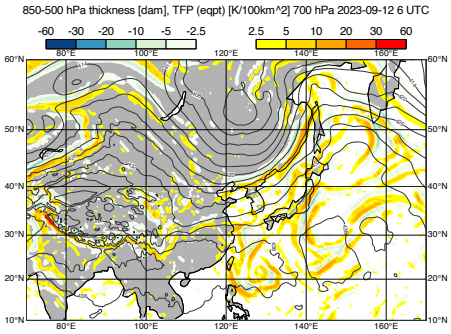

(b)

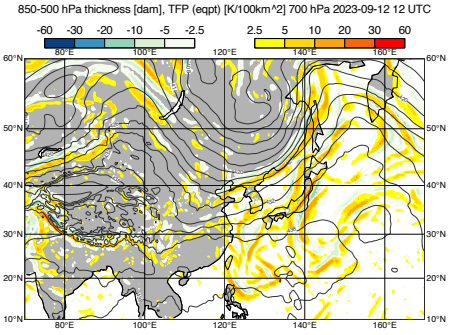

(c)

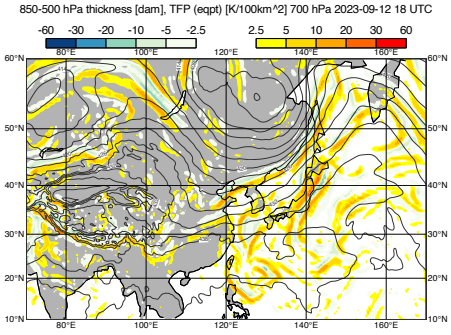

(d)

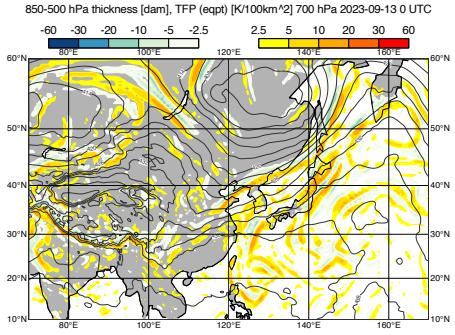

(e)

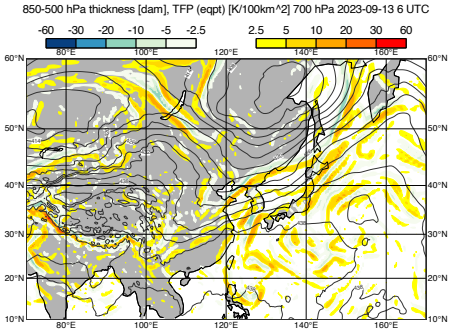

(f)

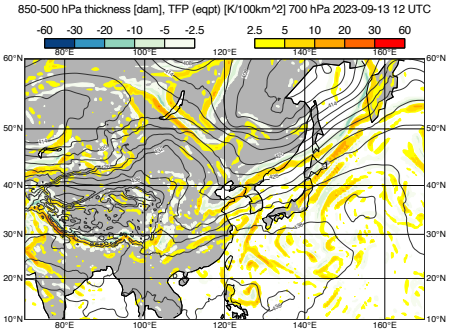

(g)

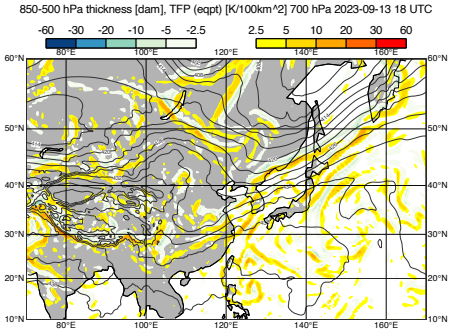

(h)

Figure S 18. The thermal front parameter (TFP) and 850–500 hPa thickness data for September 12 and 13, presented in 6-hourly intervals.

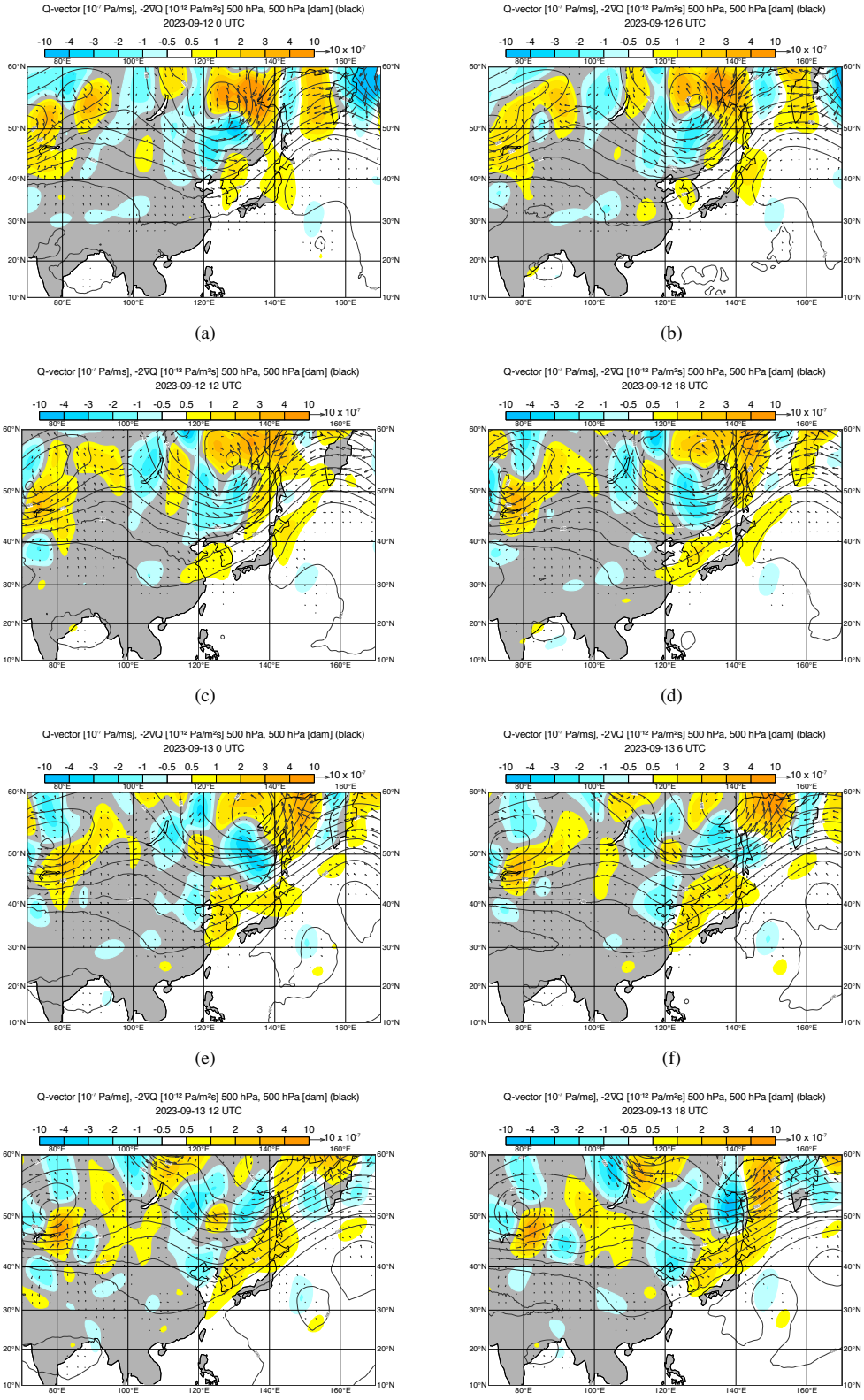

Figure S 19. Q- Vector, Q-Vector vergences, and 500 hPa geopotential data for September 12 and 13, presented in 6-hourly intervals.

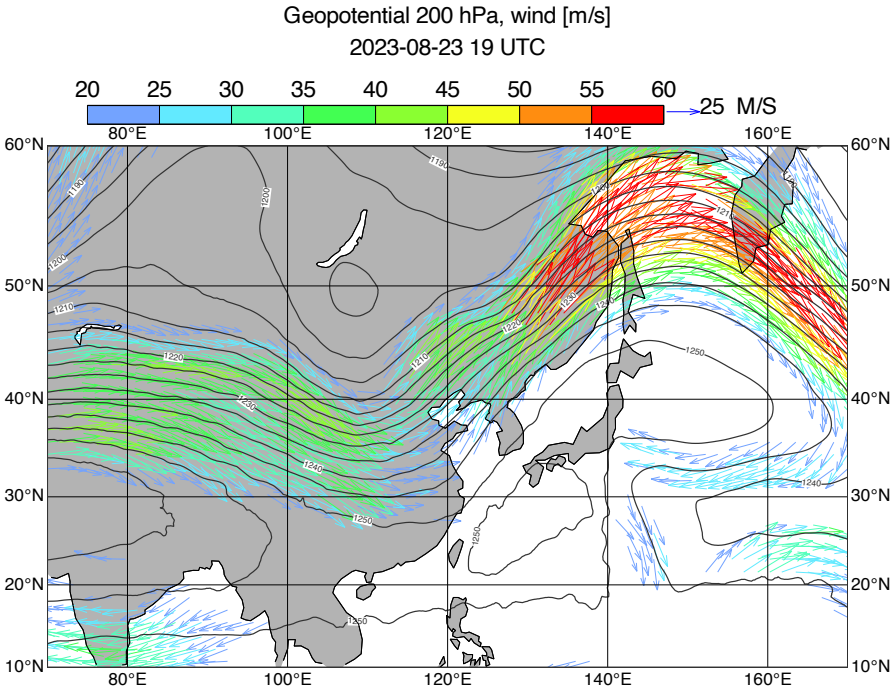

Figure S 20. Upper tropospheric meteorological situation for August 23, 2023 at 19 UTC. 200 hPa geopotential heights depicted with black lines, alongside wind vectors illustrated with colored arrows. High winds speeds (orange to red arrows) show the position of the jetstreak.